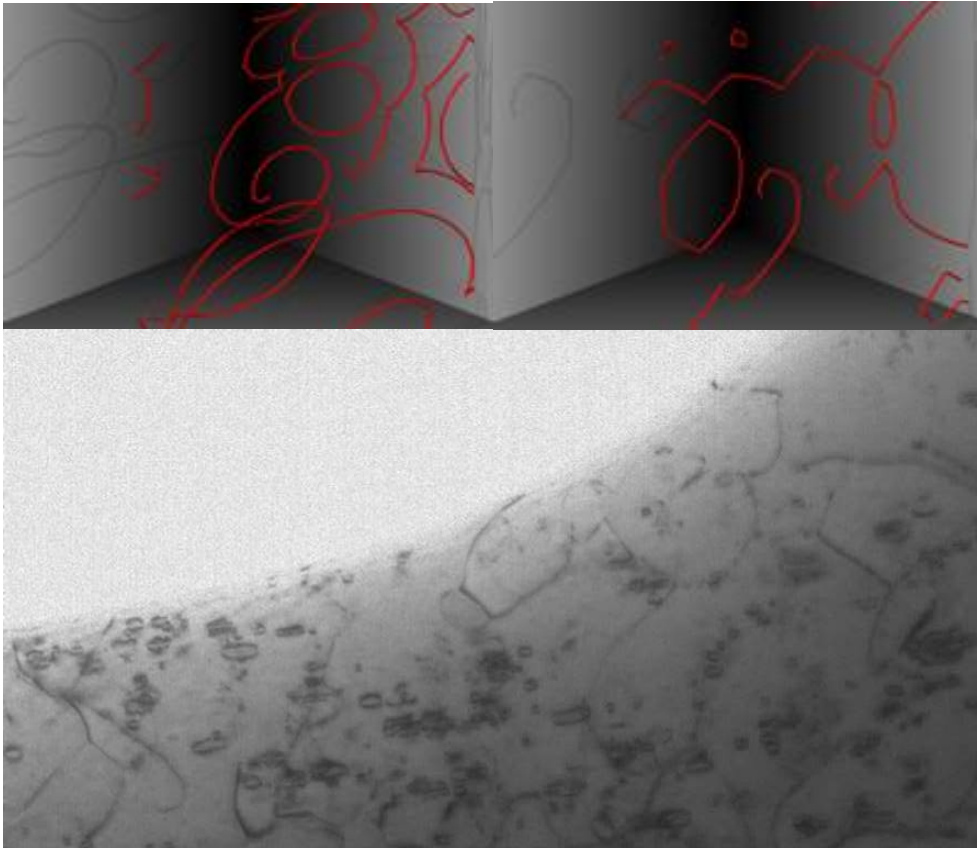


## 7 Materials and Technology

### 7.1 FUSION MATERIALS MODELLING AND VALIDATION

In 2009/2010 the fusion materials modelling and validation work has addressed a number of issues critical for the development of a knowledge-based strategy for the realization of fusion as a viable option for power generation. The need to develop mathematical methods and algorithms for modelling plasticity and predicting changes in mechanical properties due to the accumulation of radiation damage effects under fusion neutron irradiation, has stimulated extensive investigation of advanced methods for dislocation dynamics simulations.



**Figure 7.1:** Top: simulations performed using the AniDis dislocation dynamics simulation software presently being developed at Culham in collaboration with scientists from Stanford University, USA. Bottom: electron micrograph showing the microstructure of pure bcc iron irradiated with iron ions to the dose of  $\sim 7\text{dpa}$  at  $500^\circ\text{C}$  (courtesy of S. Xu, University of Oxford). Note the occurrence of characteristic sharp corners on the  $\frac{1}{2}\langle 111 \rangle$  dislocations forming the network. Most of the small loops, resulting from the agglomeration of self-interstitial atoms, have  $\langle 100 \rangle$  Burgers vectors

Earlier work performed at CCFE showed that mechanical properties of steels are significantly affected by the  $\alpha$ - $\gamma$  phase transitions, from body-centred-cubic (bcc) to face-centred-cubic (fcc) structure, occurring in pure iron at temperatures approaching  $912^\circ\text{C}$ , and at somewhat lower temperatures in dilute Fe-Cr alloys and low-chromium steels. The occurrence of a bcc to fcc  $\alpha$ - $\gamma$  phase transition is accompanied by significant changes in microscopic elastic properties of the material, which require applying full anisotropic elasticity treatment of interaction between defects and dislocations. Figure 7.1 shows that a treatment of interacting dislocations, taking full account of elastic anisotropy of the material, is required in order to achieve quantitative agreement between simulations and

experimentally observed dislocation structures forming in iron, iron-based alloys, and steels under irradiation at high temperatures.

Modelling the  $\alpha$ - $\gamma$  phase transition itself until recently represented one of the most significant challenges for modelling iron-based alloys and steels, finding a solution for which has so far proved elusive. The occurrence of the bcc to fcc structural phase transitions in pure iron, and the so-called  $\gamma$  loop in the phase diagram of Fe-Cr alloys, are the key physical phenomena determining the manufacturing and processing routes, the low- and high-temperature mechanical properties, and the type of defect structures formed under irradiation in steel developed for nuclear fission and fusion applications. Until recently, surprisingly little was known about the microscopic origin of these transitions, or about the factors determining the stability region for the fcc phase, treated as a function of temperature and chromium concentration. Work performed at CCFE has for the first time made it possible, through the development of the so-called Magnetic Cluster Expansion treatment of high temperature properties of Fe-Cr alloys, to explain the occurrence of the  $\alpha$ - $\gamma$  phase transition and to quantify the role played by the magnetic and vibrational excitations, as well as by the effects of atomic short-range order in the alloys.

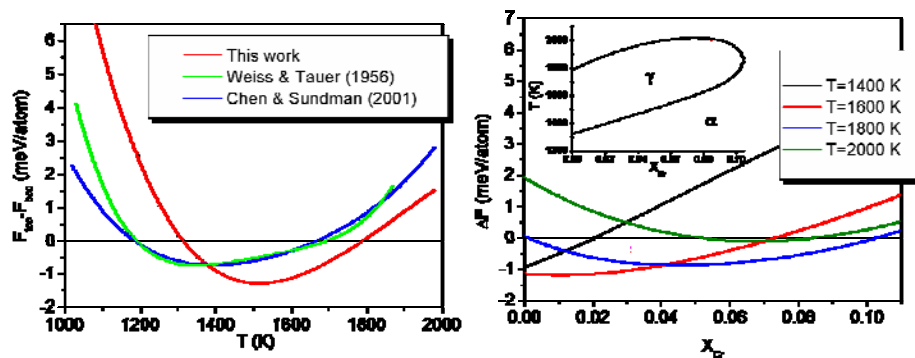


**Figure 7.2:** Difference between the free energies of fcc and bcc phases of iron plotted as a function of temperature (left) and as a function of chromium content in the alloy (right)

Figure 7.2 shows the free energy curves, evaluated using Monte Carlo simulations performed using the Magnetic Cluster Expansion treatment of interactions in the alloys, and the similar curves derived from experimental data. The fact that the new Magnetic-Cluster-Expansion-based methodology makes it possible to evaluate, at a quantitative level of accuracy, the contributions to the free energy from magnons and phonons, provides a basis for the development of rational understanding of  $\alpha$ - $\gamma$  phase transitions in iron, iron-based alloys, and steels, and opens a way to modelling micro-structural evolution under irradiation, as well as effects of radiation damage on high-temperature properties of steels developed for fusion applications.

In the design of fusion power plants and fusion experimental devices, such as ITER, tungsten is being considered for various plasma facing components because of its high melting point, high thermal conductivity, and high resistance to sputtering and erosion. As a result, tungsten is a primary candidate material for the divertor armour. These qualities also make tungsten a desirable material for use in other parts of the first wall. However, whereas the divertor armour needs only have a lifetime of around two full-power years to make fusion commercially viable, the first wall components must be typically able to withstand the fusion environment for at least five years. At these longer times, the irradiation-induced embrittlement of tungsten, which is brittle even at room temperature to begin with, will become an issue that requires serious attention.

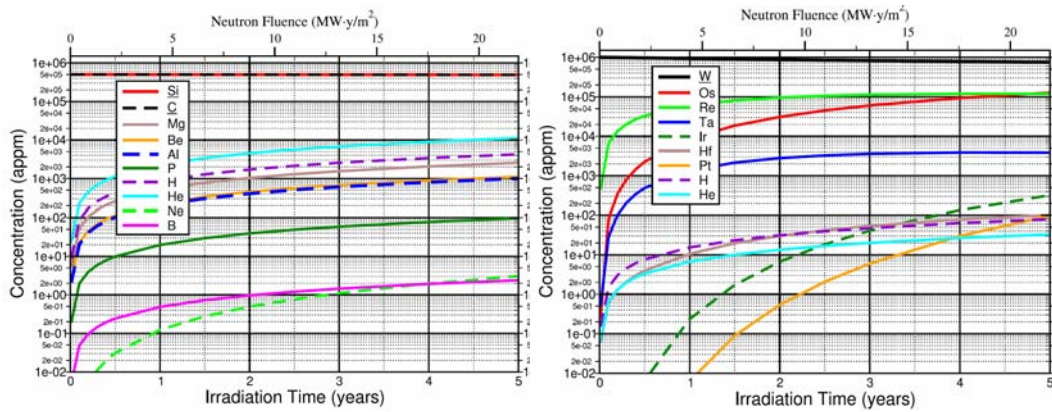


**Figure 7.3:** Plots showing the accumulation of helium and transmutation effects under irradiation by neutrons with energy spectrum typical of a fusion power plant for silicon carbide (left), and initially pure tungsten (right)

Analysis of transmutation effects in various candidate fusion materials performed at CCFE Culham and illustrated in Figure 7.3 (for more detail a reader is referred to CCFE Report - R(10)01) has shown that helium production under fusion irradiation conditions occurs at the highest rate in light materials, for example silicon, beryllium, and carbon. In heavy elements like tungsten or tantalum the helium generation rates are approximately two orders of magnitude lower, but the transmutation rates, leading to significant changes in the chemical composition of the materials, are high. For the elements from the middle of the Periodic Table (iron, chromium, vanadium) the transmutation rates, and the effects associated with helium generation, are moderate. The new data provide a quantitative basis for the assessment of candidate fusion materials against such fundamental metallurgical parameters influencing the ductility and mechanical strength of the materials, as the chemical composition of the alloys and embrittlement effects associated with the presence of helium.

Recent *in-situ* electron microscope observations, providing real-time visualisation of dynamics of defects produced by ultra-high-energy electron irradiation, or showing microstructural evolution occurring under ion beam irradiation, have revolutionised our understanding of how properties of metals and alloys change in the extreme radiation and thermal environments of a fission or a fusion power plant. The key feature of *in-situ* electron microscopy is its ability to exhibit the time-dependent dynamics of migration, interaction, and transformation of radiation defects, and to visualise the entire complexity of evolving defect and dislocation networks.

For example, *in-situ* electron microscope observations provided evidence of violation of the Burgers vector conservation law for dislocations on the nanoscale. This gave a vital clue needed for modelling microscopic processes responsible for the formation of unusual high-temperature dislocation structures in iron, and for explaining the origin of the loss of strength of ferritic-martensitic steels at high temperatures exceeding 500 °C. A particularly significant aspect of *in-situ* electron microscope observations is that they visualise the dynamics of microstructure corresponding to the limit of high irradiation dose rates, approaching 50 to 70dpa per 24h. These dose rates are similar to the 10dpa per 24h to 100dpa per 24h range of dose rates characterizing irradiation conditions in *ex-situ* ion-beam facilities. *In-situ* electron microscopy, and *ex-situ* ion-beam irradiation experiments generate similar microstructures, corresponding to a similar range of high irradiation dose rates. These dose rates are several orders of magnitude higher than the rates associated with the irradiation environment of a fission

nuclear reactor, an accelerator-driven system like the International Fusion Materials Irradiation Facility (IFMIF), or a fusion power plant.

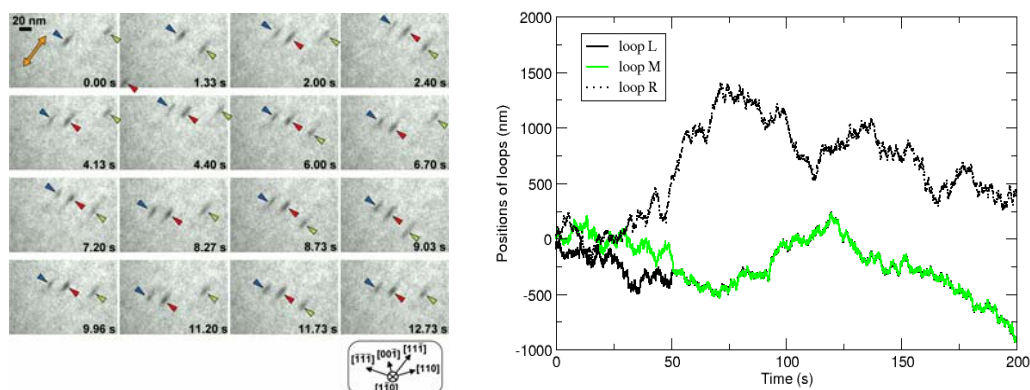


**Figure 7.4:** A sequence of electron microscope micrographs (courtesy of K. Arakawa, Osaka University, Japan) showing migrating dislocation loops formed under irradiation, and trapped by the field of elastic forces acting between the defects (left). Figure shown on the right illustrates the same phenomenon found in simulations, performed using a statistical Langevin dynamics algorithm

A new simulation algorithm developed at CCFE for modelling radiation defects as interacting mobile particles moving under the combined action of elastic forces *and* random thermal forces, has unravelled the potentially significant part played by effects of interaction between the defects, and the need of including the treatment of these interactions in models for microstructural evolution of radiation induced defect structures found in ion-beam irradiation experiments. The new results show that the treatment of high irradiation dose rate effects characteristic of ion beam irradiation experiments, and not characteristic of either fission reactor experiments or future IFMIF tests, needs to be included in the microstructural evolution models, to fully exploit the potential of ion beam irradiation facilities for testing and characterization of radiation stability of candidate fusion materials.

## 7.2 NUCLEAR DATA AND CODES FOR TRANSMUTATION-DECAY MODELLING

High quality activation data and transmutation–decay inventory codes are of fundamental importance in the development of new nuclear technology such as fusion energy. In the steps towards an operational fusion power plant the behaviour of new materials and components need to be simulated in these intense neutron fields so that one may predict the levels of activation necessary, for example, to calculate dose budgets for operations and maintenance, to predict waste inventories for decommissioning strategies, and to estimate effects such as material swelling and embrittlement. Such simulations are required to design, optimise and ultimately select promising candidate materials for components which require further qualification and testing in high neutron flux irradiation fields, such as the materials testing facility IFMIF and component testing facilities (CTF).

The CCFE Neutronics and Nuclear Data Group maintain and actively develop the capability and tools required to perform such simulations. One of the key areas of expertise lays with the production the European Activation File (EAF), which has been developed and continuously improved for more than 20 years. This year the latest and most improved version, EAF-2010, was produced at CCFE using the SAFEPAQ II tool as part of a contract partly funded by F4E. The file is a component part of the European Activation System (EASY), which also includes the transmutation–decay inventory code FISPACT and has been adopted for use

in many nuclear applications, notably for ITER related calculations. It includes data for neutron-induced reactions up to 60MeV which covers the neutron spectrum energy range required for IFMIF and other high energy field research facilities. EASY also includes data and tools to calculate activation due to deuterons and protons.

The various components of EAF-2010 are shown conceptually in Figure 7.5, which shows the number of target nuclides, reaction cross sections and the decay nuclide data present in the file. Targets and decay nuclides are plotted in Figure 7.6. Methods to evaluate cross sections with the best available experimental data have been used. Identification of important reaction cross sections for nuclear technology applications have been developed using SAFEPAQ II and EASY tools to allow resources to be focussed on improving data where it matters the most. Validation processes are essential to our data and have been applied to reactions with supporting experimental data. In addition, methods to improve data within EAF that have been derived from theoretical model simulations by means of statistical analysis of cross section methods (SACS) continue to be developed and applied.

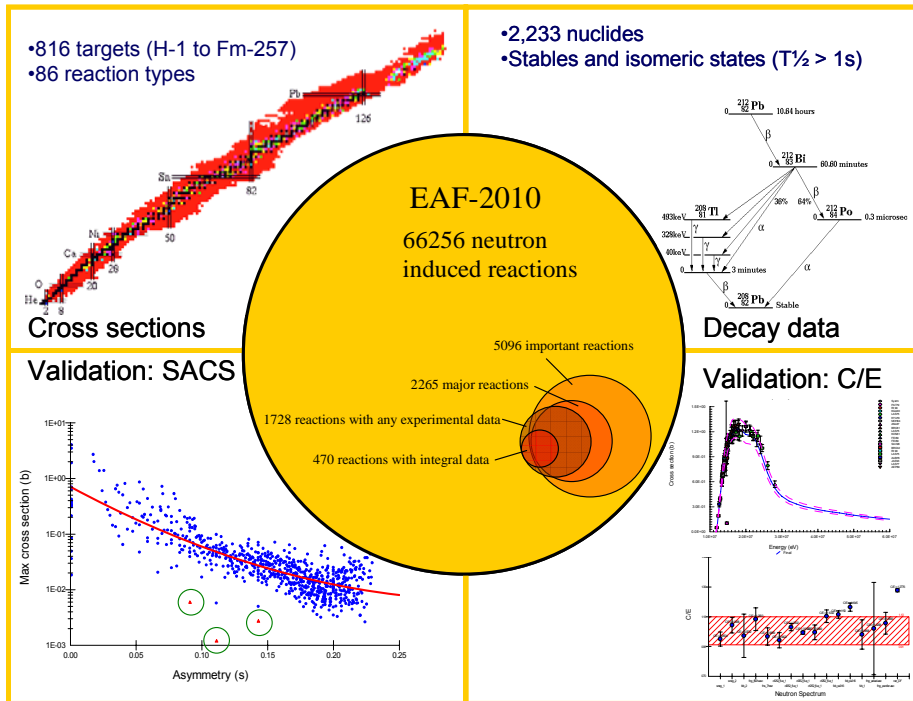
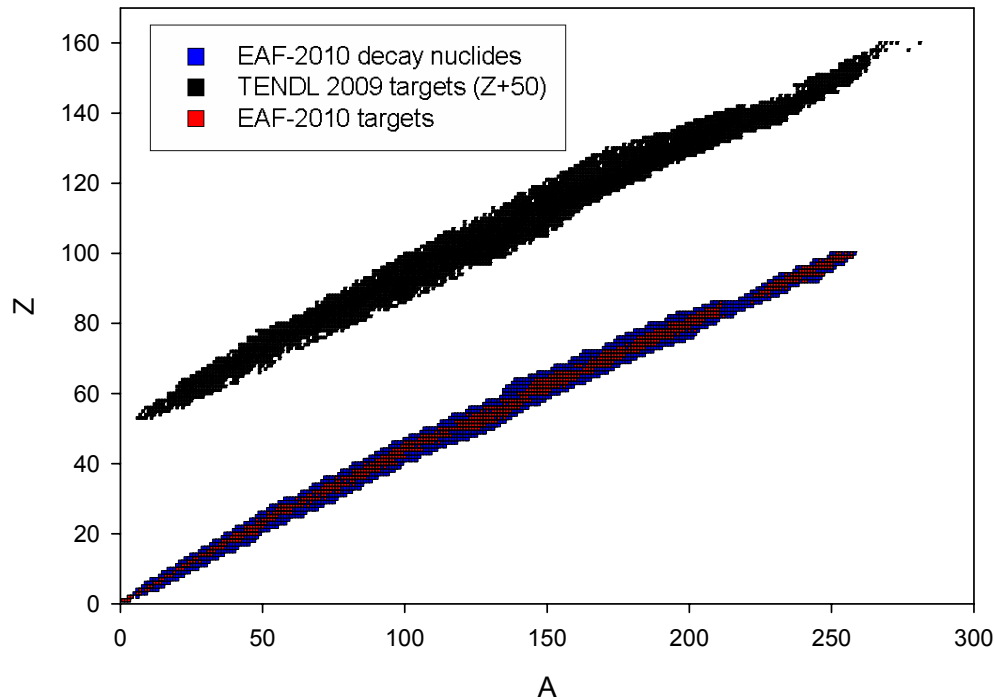


Figure 7.5: EAF-2010 components overview



**Figure 7.6:** Atomic mass ( $A$ ) versus proton number ( $Z$ ) plot of EAF-2010 targets and decay nuclides. Model derived TENDL-2009 targets are shown with  $Z=Z+50$  to aid comparison

## 7.3 PLASMA FACING MATERIALS

### 7.3.1 PREPARATION FOR THE JET ITER-LIKE WALL

At the end of October 2009 plasma operations in JET were suspended to allow the installation of the ITER-like Wall (ILW, see Chapter 3). The plasma-facing surfaces in the vessel are being changed to beryllium (Be) or tungsten (W) from predominantly carbon, which requires the removal of all the wall and divertor tiles that have been in the machine for the past years (over 4000 tiles), cleaning the vessel, and replacement with a mixture of bulk Be, Be-coated inconel, W-coated carbon and solid W tiles. Major objectives of the ILW are to measure the erosion, deposition and fuel retention with the new metallic plasma-facing surfaces, for comparison with the previous carbon wall. Measurement of erosion is a particular challenge, as it requires very accurate measurement of the tile surface before and after exposure in JET. These measurements will be made at two levels: for erosion of a few microns, and for erosion of  $>10$  microns. In order to measure erosion of just a few microns, special marker tiles will be distributed around JET. These tiles are coated with an interlayer of a material which can be easily identified by Ion Beam analysis, then a top layer of similar material to the substrate, as shown diagrammatically in Figure 7.7; for Be wall tiles Ni is used as the interlayer, and for tiles with W surfaces in the divertor Mo is used. The amount of erosion is determined by analysing how much Be (or W) remains above the interlayer after exposure in JET.

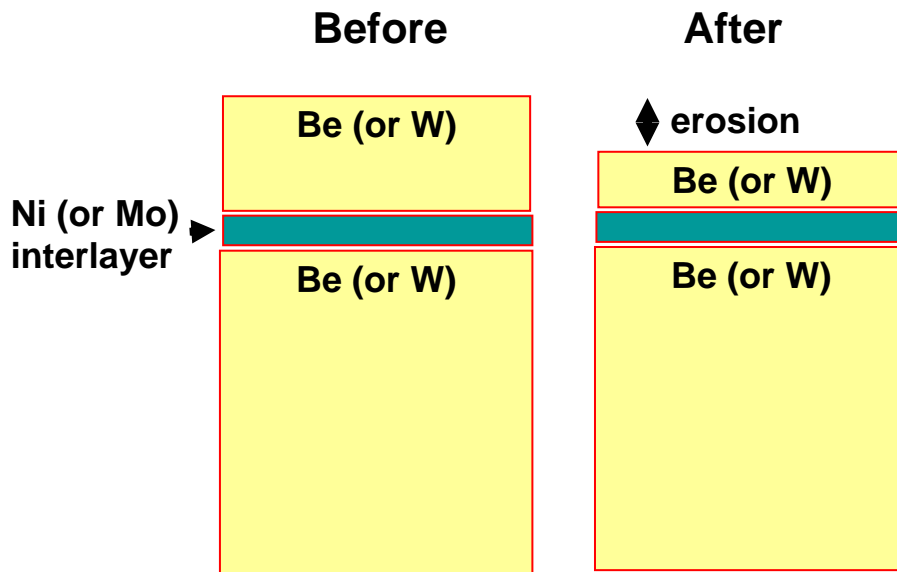


**Figure 7.7:** Schematic of the marker tiles. A layer of material similar to the substrate is deposited over an interlayer of a dissimilar material (chosen to be easily distinguished by analysis and thermally stable at the operating temperatures)

Of course, if the erosion is much greater than a few microns, the marker layer will have completely disappeared. Therefore, the marker tiles are also measured mechanically with a tile profiler (shown in Figure 7.8) that maps the surface of the tile before and after exposure in JET. Although the accuracy of individual measurements is 0.5 microns, reproducibility in positioning the tile on the profiler limits the achievable accuracy in mapping the surface to ~10 microns.

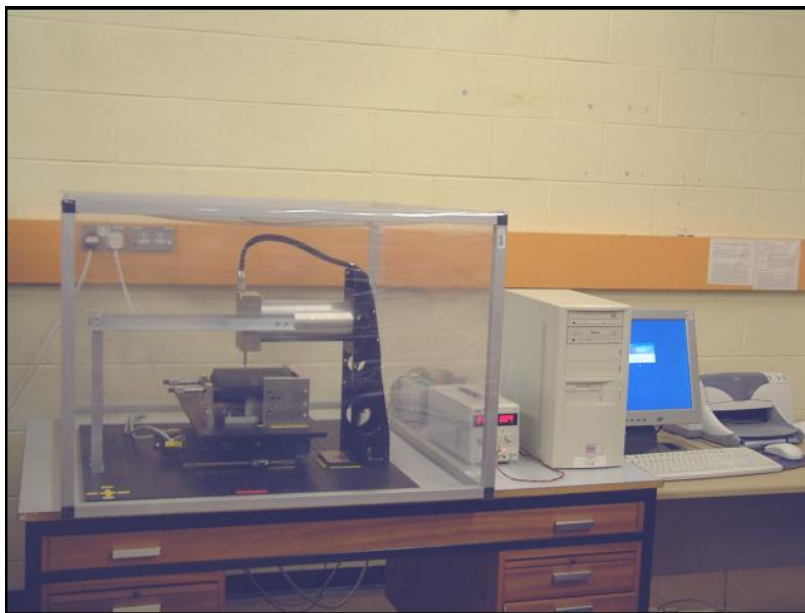


**Figure 7.8:** The tile profiler used to map the tile surface before and after exposure in JET to determine erosion

Marker tiles for the divertor and the wall have been produced and are being analysed ready to install as part of the ILW.

### 7.3.2 COLLECTION OF JET IN-VESSEL DUST

An important issue for the safety case for ITER is the nature and amount of dust that will accumulate during operation, so ITER are very interested in the dust that is produced in JET. The shutdown for the installation of the ILW is a unique opportunity to collect the dust from within JET. The majority of dust in JET comes from the break-up of material that has been eroded by the plasma and re-deposited as surface films, and the majority of this ends up in the divertor. Therefore, collection of dust from the divertor was incorporated into the shutdown plan. The divertor is cleaned of loose material at each shutdown by Remote Handling using a specially adapted cyclone vacuum cleaner; most of the dust precipitates into a pot which can be changed under the cyclone. For this shutdown the cleaning has been done in a much more controlled way so that the quantity of dust in different regions of the divertor can be assessed. The vacuuming activity was broken down into six stages, vacuuming each in turn and with a different pot for each stage.. With reference to Figure 7.9, the stages are: the vertical outer divertor tiles plus the Load Bearing tile (LBT) – Stage 1; the vertical inner divertor tiles – Stage 2; the divertor carrier ribs – Stage 3 (carried out manually in the controlled area attached to the torus); the outer divertor floor tiles – Stage 4; the inner divertor floor tiles – Stage 5; and the divertor structure, including inner and outer louvers – Stage 6. In case not all the dust gets collected in the pot, on a number of occasions the cyclone itself and the connecting pipework and filters were also changed and any dust remaining in these areas will be added to the appropriate pots. The pots etc will be stored safely until the end of the shutdown, whereupon the dust will be weighed and will then be available for characterisation. A number of divertor tiles and tiles from areas of deposition in the main chamber that were deliberately *not* vacuum cleaned will also be available for analysis of dust and flakes present on the surface.

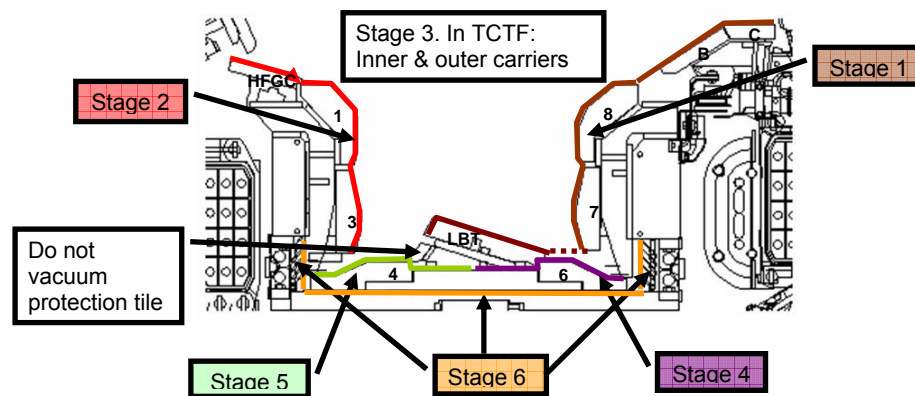


**Figure 7.9:** Staging of the collection of dust and flakes from the divertor during the shutdown to install the ILW

### 7.3.3 CLEANING OF MIRRORS EXPOSED IN JET

Many of the diagnostics in ITER will be viewed via mirrors in the divertor and in the main chamber. Mirrors made from stainless steel (SS) and molybdenum (Mo) – candidate materials for the ITER mirrors – were exposed to 127,000s of plasma operations in JET from 2005-2007. The mirrors, located in the divertor and at the outer mid-plane of the vessel, were found to be covered with deposits up to 10 $\mu$ m in thickness [M Rubel et al, J. Nucl. Materials 390-391 (2009) 1066], and all showed greatly reduced reflectivity as shown in Figure 7.10. If the mirrors can be cleaned in situ, for example with a laser, use in ITER may still be possible, so a selection of these mirror samples with well adhered deposits (i.e. not flaking) of

up to a few hundred nm in thickness have been cleaned using a laser system developed at CEA, Saclay.

The trials were performed in the JET Beryllium Handling Facility (BeHF) using a scanning laser with a wavelength of 1064nm, spot size diameter of 150 $\mu$ m and repetition rate of 20kHz. The 1cm<sup>2</sup> mirror surfaces were cleaned using a range of different laser fluences and number of scan repeats at a rate of 0.18m<sup>2</sup>/hour/scan to assess the best parameters for cleaning. The damage thresholds of the mirrors by the laser were established by a series of trials performed at the CEA, Saclay; multiple pulses in the same position were shown to result in lowering these thresholds by ~50%. Keeping below the 'one pulse' energy density threshold during the laser cleaning trials it was possible to bring about a noticeable change to both the SS and Mo mirror surfaces – which was assumed to be removal of deposit – by repeating scans up to 20 times in some cases. Following the laser cleaning further reflectivity and ion beam analysis of the mirror surfaces were performed. Reflectivity measurements show that the recovered reflectivity was generally better in the infrared than the visible spectrum, with recovery of up to 90% of the reflectivity deficit being obtained for both Mo and SS samples, as shown in Figure 7.10. In the visible spectrum recovery towards the original reflectivity was as low as less than half the deficit at a wavelength of 400nm rising to 70-80% of the deficit (for Mo) or around 65% of the deficit (for SS) at 800nm. From ion beam analysis it was found that a trace amount of deposit remained on the mirrors after the trials, and Scanning Electron Microscopy showed that there was some microscopic damage to the surface at each laser pulse. Clearly some improvement is required, e.g. by further optimisation of the laser parameters. However, if a reasonable reflectivity can be restored, and it proves reproducible with repetitive cleaning, then a mirror system may prove viable for ITER.

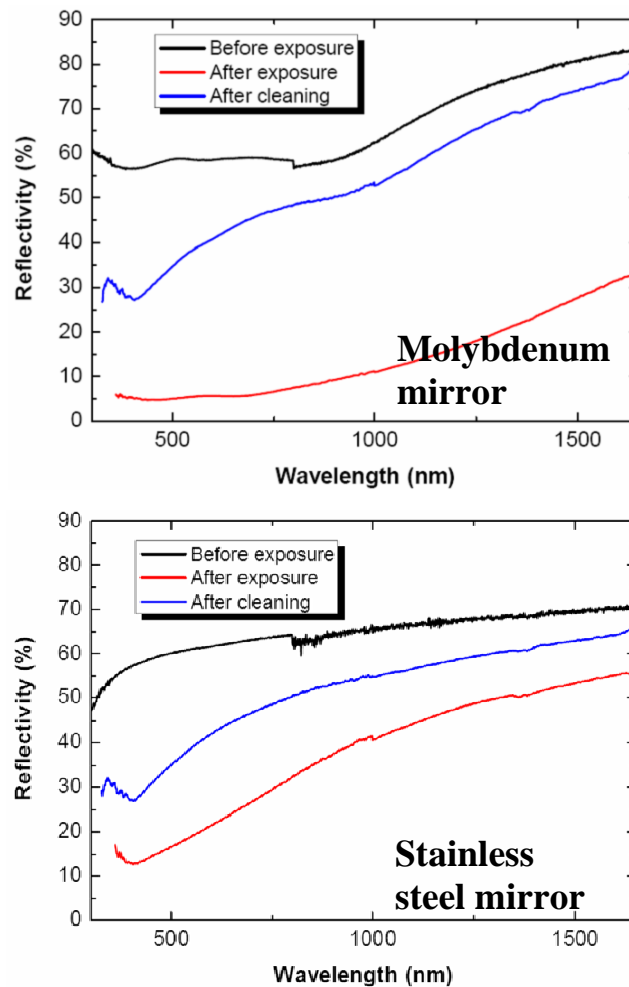


**Figure 7.10:** Reflectivity for mirror samples as received, after exposure in JET 2004-07 and after cleaning with a laser

## 7.4 TECHNOLOGY

### 7.4.1 DEMO AND POWER PLANT STUDIES

The design of DEMO remains to be determined and even its mode of operation is presently uncertain. In particular, there remains a debate between a truly steady-state device which, in a tokamak design, needs efficient and reliable current drive systems, and the alternative of a pulsed device in which the electrical output is maintained in steady-state by the use of energy storage technologies. The design of these two options differs by much more than the presence or absence of the current drive and energy storage systems of course, and this has been investigated in more detail this year.

#### A Pulsed DEMO

In a pulsed device, the design is simplified by the reduced need for a current drive system, but complicated by the energy storage system and, more importantly, by the way that many components experience pulsed loads, from heat flow and from electromagnetic forces. These engineering aspects of a pulsed device may, at first glance, make it an unattractive option for DEMO, but

this needs to be quantified and compared with the cost and recirculating power fraction of the continuous plasma current drive system. In order to gain insight into these problems, several studies have been carried out to look at the effect of pulsing on the first wall, the magnets, and the corresponding needs for the energy storage system.

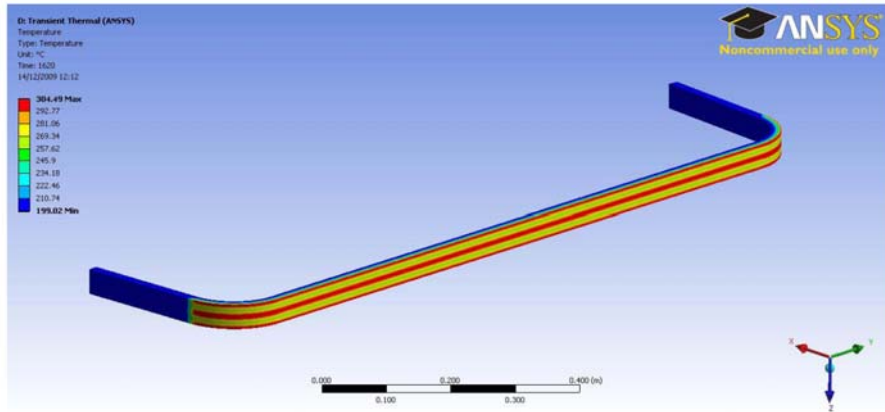


**Figure 7.11:** Model of a first wall segment used in analysing the cyclic fatigue expected in a pulsed version of DEMO

Figure 7.11 shows a model of a first wall segment that has been used in a preliminary study of a pulsed device, with heat load falling on the surface in a pulsed manner. Although this work is ongoing, initial results suggest that, depending on the details of the material properties and the heat pulses, the first wall lifetime may be restricted to values which would be considered too small for DEMO. Better data and further analysis will be needed to determine whether this feature of a pulsed device will be very limiting but it appears possible that the resilience of the first wall to pulsed heat loads has the potential to seriously limit the design of DEMO. A key uncertainty at present is the creep-fatigue behaviour of the candidate wall materials in conditions of high neutron irradiation, sustained (but inconstant) high temperature and substantial stresses, both near-continuous and cyclic.

In a related study, modelling the magnets in a pulsed version of DEMO has been carried out and early results are now available. The purpose in this case is to characterise the results in a way that is sufficiently simple to allow implementation in a systems code. In this way, the effect of cyclic stresses on magnets can be incorporated in the initial conceptual design of DEMO, through systems analysis, rather than analysed after the concept is fixed. Again this work is ongoing but early results suggest that pulsed operation will force the magnets to be operated at lower levels of magnetic field, hence degrading the overall machine performance. As with the first wall, the effect is to produce a different optimum design of DEMO which will provide much more reliable information for the comparison between the pulsed and steady-state DEMO options in terms of overall cost of electricity generated.

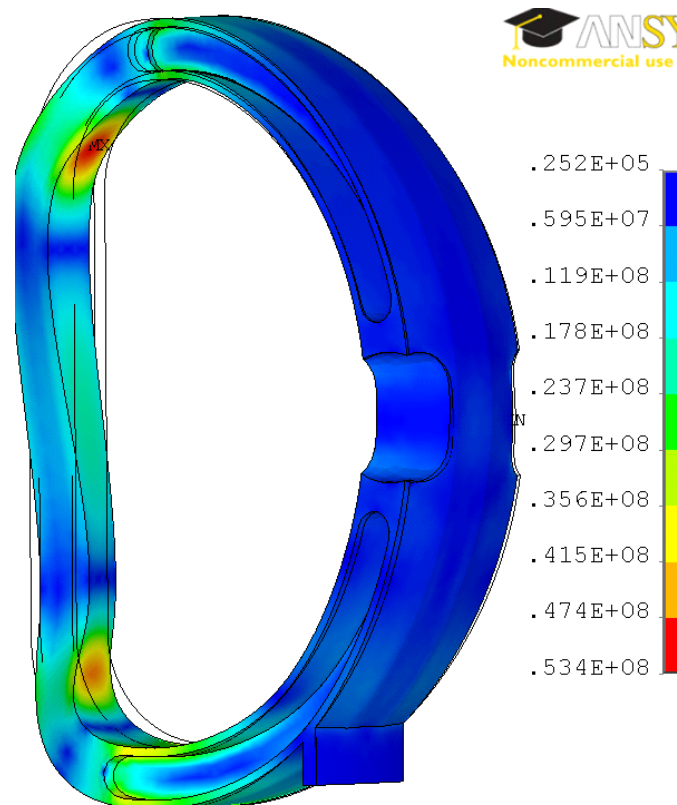


**Figure 7.12:** Toroidal field coil model used to analyse cyclic fatigue due to pulsed operation of DEMO. The colours show the Von-Mises stress in the coil case

Apart from the reduction in performance due to pulsed stresses, there is the need in a pulsed DEMO for energy storage to smooth the power output to allow a continuous supply of electricity to the grid. There has been a lot of work in this area over recent years, primarily related to renewable technologies, and we can now consider the application of such systems to a fusion plant. Although the fusion plant is expected to be a much higher power system, the time for which the power output needs to come from the energy storage system (the 'dwell' time between pulses) is much shorter than for renewable technologies, such as solar thermal. The ratio is likely to be one of several minutes, for fusion inter-pulse dwell, compared to 8-12 hours, for overnight energy storage to smooth out a solar thermal supply. This means that, in terms of energy stored, a pulsed DEMO device would only need an energy storage similar to those that are in use or close to demonstration already. In terms of power production, however, they would be quite different and further work is needed in this area. Figure 7.13 shows the result of applying such an energy storage system to pulsed operation of DEMO, showing the total fusion power, the electrical power to the grid, and the temperature variations of a molten salt energy storage system, comparable to one operational in an existing solar thermal plant. This appears to offer a surprisingly cost-effective option for pulsed DEMO and suggests that it is the other aspects of pulsing, related to the first wall heat load and magnet stresses, as well as other issues such as pulsed neutronic loads, that will be the determining factors in pulsed designs.

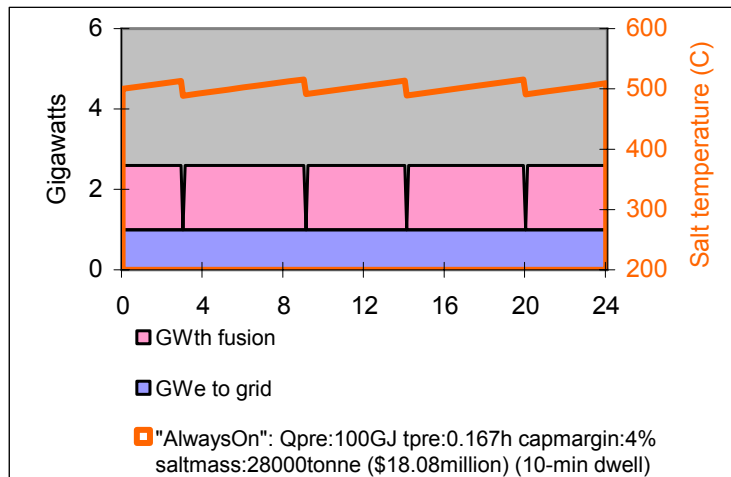


**Figure 7.13:** Modelling the use of a molten salt storage system to smooth the output power from a pulsed version of DEMO suggests that this is a reasonably cost-effective solution

This modelling of an energy storage system suggests that we can estimate the optimum dwell time, during which no power is produced, for a pulsed version of DEMO. The energy storage system becomes more expensive as the dwell time increases, however at the same time, other aspects of the design become cheaper – here we consider the power supplies needed to recharge the central solenoid coil which is responsible for driving the plasma current in the pulsed design. Whilst this is only an approximate characterisation at this point, it already gives interesting results. Using the costs of the molten salt energy storage system and estimates of power supply costs, Figure 7.14 shows the way in which these vary with the dwell time, and suggest that a down time of around ten minutes is the optimum. At shorter times, the cost of the systems needed to restart the plasma is higher, at longer times the cost of the energy storage system is higher. There are, of course, many elements to this that have not been accurately included but it is an important result nonetheless.

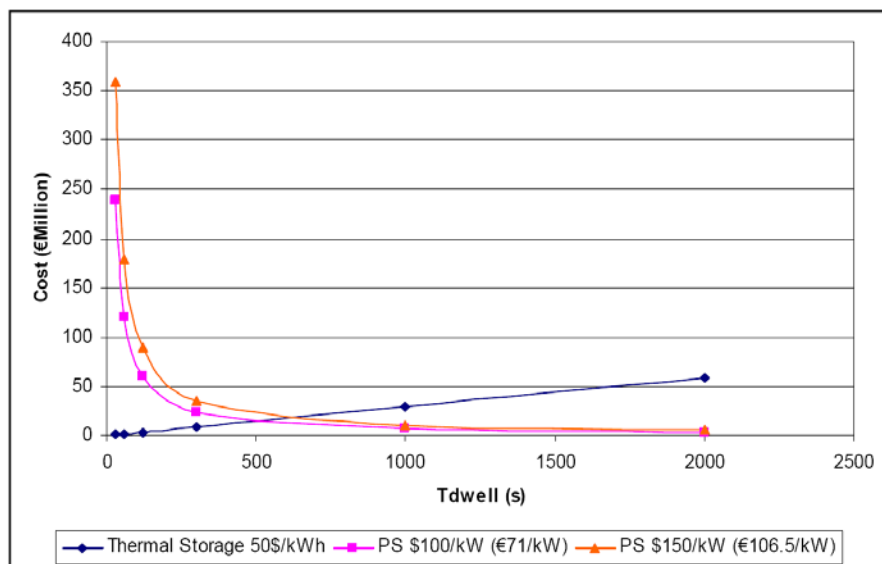


**Figure 7.14:** In a pulsed device, the balance of cost of power supplies needed to restart the device and the cost of energy storage to smooth electrical output, suggests an optimum design with a dwell time of ten minutes or more

## B Steady-state DEMO

In addition to developing models of a pulsed DEMO design, work has continued to determine more of the details of an optimised steady-state device. Figure 7.15 shows the result of taking a systems studies design and carrying out an equilibrium analysis. This attempt to produce a real equilibrium based around actual coil positions emphasises one difficulty in DEMO and in power stations, that there is expected to be substantial distance between the plasma and the poloidal field coils, to allow for the blanket, shield, vessel and toroidal field coils. This work has then been used to study, in quite some detail, the current drive requirements using negative ion neutral beams, and the stability properties of the resulting equilibrium current profile. For the first time in our studies, this has been an iterative process where detailed analysis of the stability has suggested changes to the neutral beam system which allow higher device performance. The results are not given in detail here but a simple example is that the initial proposal to use neutral beams above 1.5MeV was found not to be beneficial as the resulting current profile was much more peaked than the optimum suggested by the stability analysis, leading to an overall degradation in the performance.

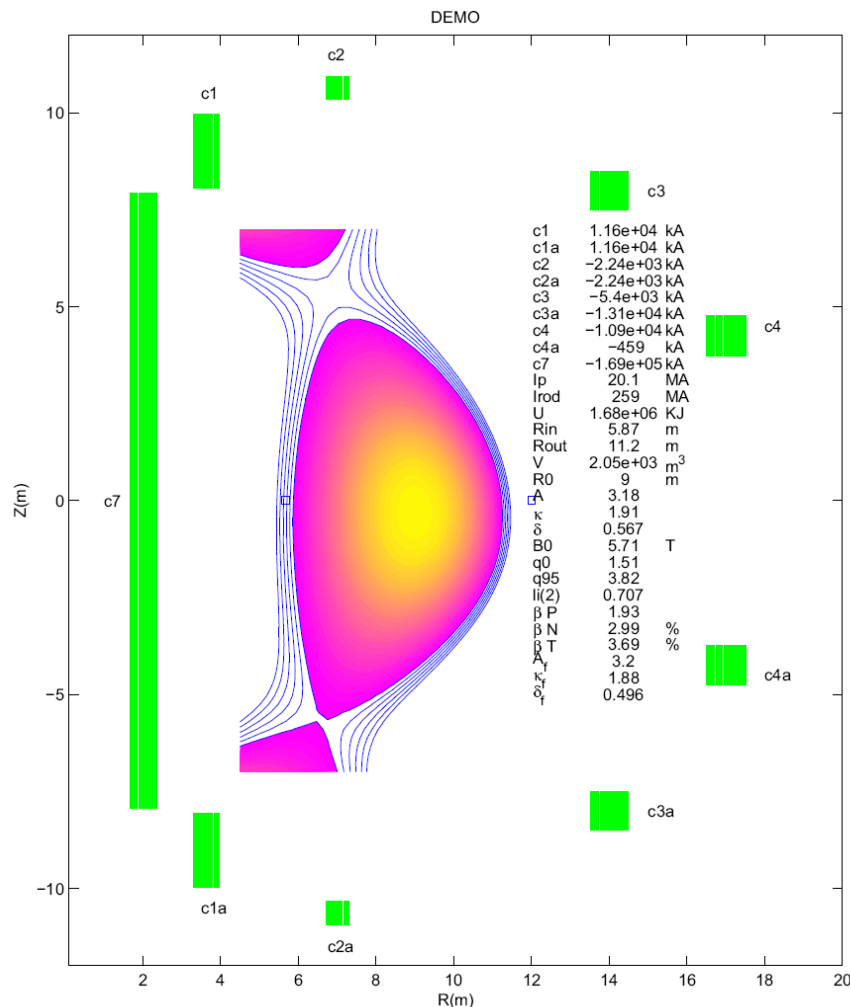


**Figure 7.15:** Equilibrium analysis for a steady-state DEMO device, attempting to use realistic coil positions. This equilibrium is then used for the current drive and stability analysis

## C DEMO heating and current drive

Both the pulsed and steady state DEMO devices will require additional heating to achieve a burning plasma and, for the steady state option, significant power is required for non-inductive current drive. The additional heating power is typically of the order 100MW and for steady state current drive the power required may be of order 250MW. There are four possible systems considered: neutral beam (NB), electron cyclotron (EC), ion cyclotron (IC) and lower hybrid (LH) but the efficiency and location of coupling to the plasma favours NB for H&CD with EC being used for plasma control and IC and LH contributing to start-up. It is therefore possible to define a number of exemplar power waveforms for each of the systems, assess the operational implications for the technology and identify and prioritize necessary R&D.

Analysis of the present performance of the four systems showed the need for R&D in several common areas such as materials, engineering analysis and power efficiency. This latter is particularly important for steady state (less so for pulsed) operation, particularly for NB. The study shows that a simultaneous optimisation of neutralization, transmission and current density is required to achieve wall plug efficiency above 50% (Figure 7.16), requiring significant R&D in the physics and technology of neutralization, beam optics and negative ion production, particularly to replace the 24kg of caesium that would be consumed annually using ITER NB technology.

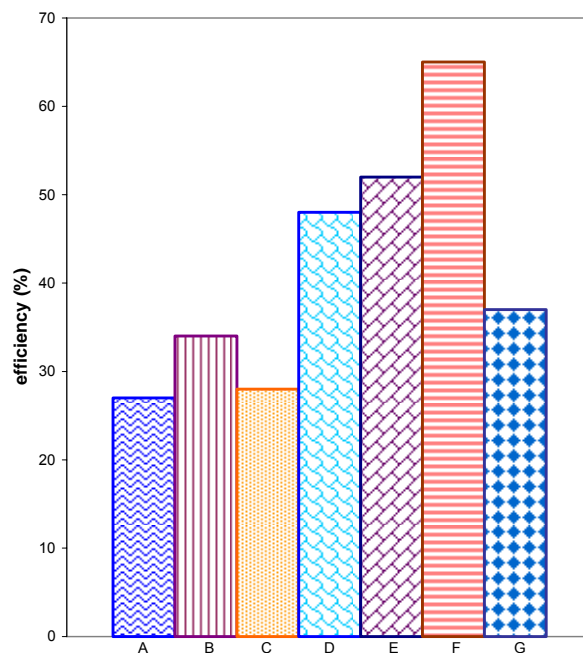


**Figure 7.16:** Wall plug efficiencies for different NB options: A standard ITER 5mrad; B ITER 3mrad; C as A with 50% increase in current density; D as A but with plasma neutralizer; E ITER 7mrad and photoneutralizer; F ITER 3mrad, photoneutralizer and 50% increase in current density; G as A with energy recovery

All systems will need to operate for longer pulse lengths than on present tokamaks and for NB current drive a single pulse could be weeks long. One consequence is that peripheral beamline components, normally un-cooled, may attain significant temperatures under the action of relatively low heat flux (for instance  $1\text{kWm}^{-2}$ ). This implies that for long pulse operation, thermal analysis of an individual component in isolation is inadequate as the heat sources and sinks of the environment must be included. This will significantly complicate engineering design in future and, indeed, this work showed an inadequacy in the

thermal analysis of the ITER absolute valve under long pulse conditions which is being rectified. Modulation of the neutral beam power is useful for plasma control and this will dictate the minimum unit size of beam source. One concern is the area occupied by the NB ports as this represents a loss in the tritium breeder blanket area. The beam sources could, in principle, be clustered at a relatively small number of ports (ie. have a high 'stacking density'). There is a limit to the number of high-voltage units which can be close-packed together (to satisfy voltage stand-off requirements). A preliminary optimisation study has shown that there is little gain in striving for a high stacking density and that the total port area used for a typical power plant design is less than 1% of the blanket area.

For the RF systems, the technology is reasonably well developed but the major R&D issue is coupling to the plasma; present efficiencies are either too low or too limited to the outer region to have significant impact on the current drive mix.

#### D Negative ion production studies

The significant R&D identified in the H&CD DEMO study will require investment in a number of test stands and a shortfall of suitable NB facilities has been identified. To contribute to the NB development programme, the EFDA JET Neutral Beam Test Bed (NBTB) was successfully converted to extract negative ions from a standard JET PINI source. This required the reversal of polarity of the HV power supply to provide 80keV negative beam voltage and the inclusion of additional auxiliary extraction and electron suppression supplies in addition to new single aperture accelerator grids incorporating electron control features.

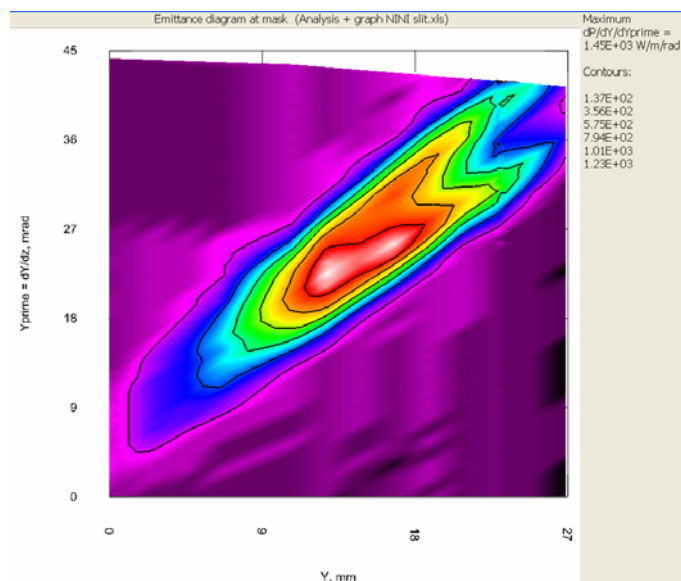


**Figure 7.17:** Thermo-graphic emittance image of  $H^-$  beam extracted on EFDA-JET Neutral Beam Test Bed

The beam profile was measured thermo-graphically using an infra red camera and target technique specially devised for the diagnosis of low power beams. The results indicated beam currents between 3mA and 10mA in  $H^-$  at energies around 40keV, corresponding to a current density of  $20\text{Am}^{-2}$  to  $65\text{Am}^{-2}$ . Unfortunately there was insufficient time in the programme to optimize this value which is slightly lower than might be expected from a pure volume source. The technique also allowed the beam emittance diagram to be obtained (shown in Figure 7.17); the bifurcation in the upper right is common in negative ion emittance diagrams although its cause is unknown.

This demonstration, the first negative ion beam extracted at Culham since 1992 shows that the JET NBTB could become a useful facility for the negative ion beam R&D programme necessary for DEMO. In particular, the prospect of conducting research at high powers relevant to fusion NB would make it a valuable tool for the future.

## 7.4.2 SOCIO-ECONOMIC STUDIES

### A Fusion in energy scenario models

Work on the modelling of future energy scenarios has continued, in collaboration with EFDA partners, using the EFDA/TIMES scenario modelling. This work has proceeded to the point where validation and comparison with other studies has been carried out and where the possible implication for fusion's future role can be investigated. Figure 7.18 shows an example of the use of the EFDA/TIMES model in which fusion is assumed to be available from 2050, at a reasonable cost, but the development of a second generation of fusion plant is not available. At the same time it is assumed that carbon emissions are restricted so that the atmospheric concentration of CO<sub>2</sub> reaches 650ppmv (equivalent) by 2100, a value often considered by climate experts to be too high. The result of such analysis is, as expected, to produce a major role for non-carbon energy systems, indeed in the second half of the century, the global electricity production is entirely produced by non-carbon sources, including fusion. This is in no sense a prediction of the future, but is an illustration of what may happen under the specific assumptions.

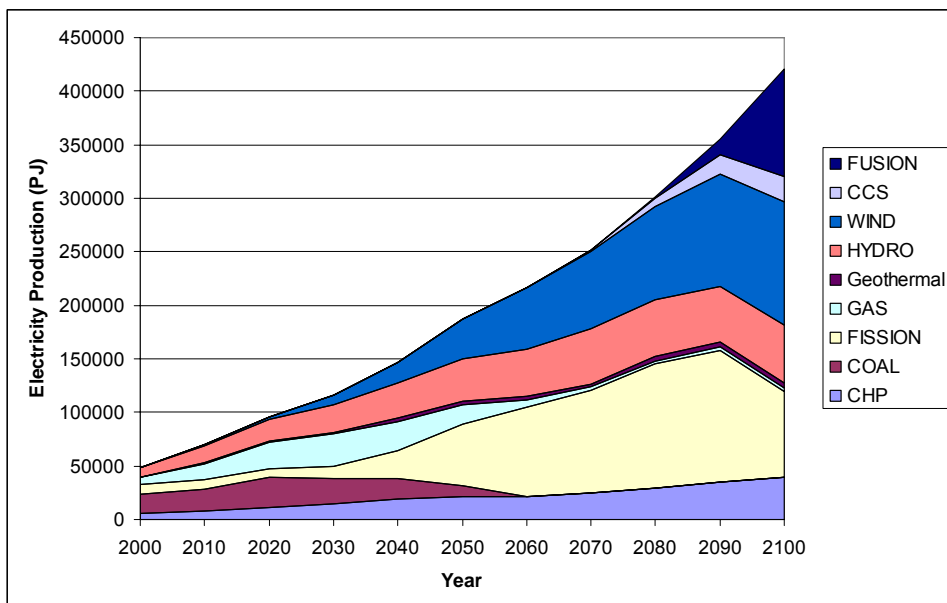


**Figure 7.18:** Scenario model of the future global electricity supply out to 2100 using the EFDA/TIMES model under the assumed restriction of atmospheric carbon dioxide concentration to 650ppmv equivalent

Having a stable reference model using EFDA/TIMES, we can use that to explore the results of changing the fusion assumptions (the outcome of the fusion development programme). In other words we can look at the implications for fusion power of different outcomes of the fusion programme. There is a wide range of results available but only one is shown here – the effect of different normalised beta (a measure of the plasma pressure) on the fusion market share in 2100, under different assumptions about the atmospheric carbon restrictions

given in Figure 7.19. These results show how the role for fusion depends strongly on the external conditions such as carbon constraints as well as on the outcome of the fusion development programme. If a strong reduction in atmospheric carbon is needed then there is a larger role, over the century, for non-carbon sources including fusion and it appears that moderate fusion performance is sufficient to allow a large role for fusion. Conversely, a more moderate carbon target results in a more modest role for fusion unless there is a much more ambitious target for fusion performance.

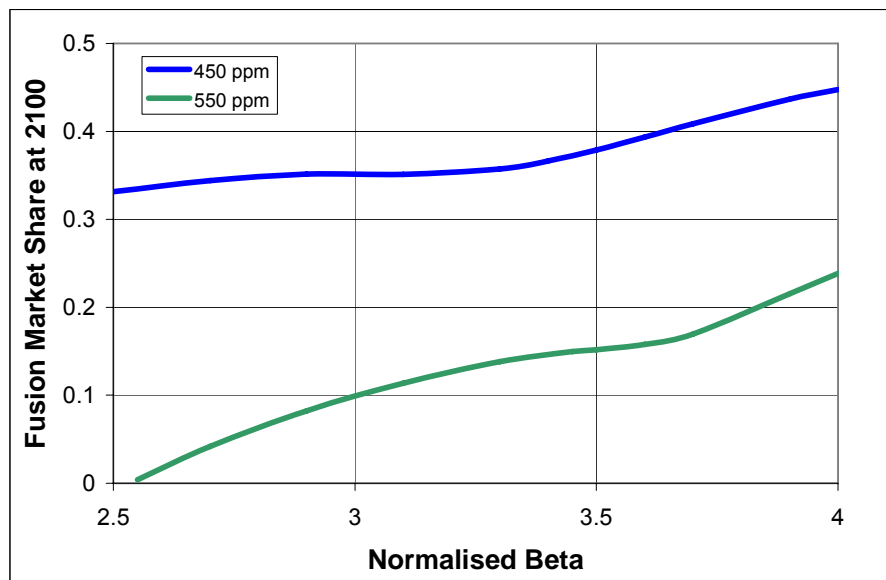


**Figure 7.19:** The potential share of global electricity produced from fusion in the year 2100 at different levels of carbon constraint and normalised beta

## B Non-electric applications of fusion

Work has continued on the possible use of fusion for purposes other than producing electricity. There are many options, ranging from hydrogen production for transport through to incineration of nuclear waste. Recent work has concentrated on production of gases, including hydrogen.

There has been effort to look at how fusion is coupled to other areas of existing and future markets, and of particular interest is the coupling to other energy systems. If fusion is to be used to produce industrial gases there are a number of new and important options. For instance, it is known that there may be a future scarcity of helium resources which may drive fusion to use high temperature superconductors. An alternative is to use air separation units to produce a wide variety of gases, including helium, but in doing so, large quantities of oxygen would be produced which does not, today, have a market demand. Similarly if fusion were used to produce hydrogen, there would also be a large production of oxygen. This large production of oxygen may have a market in a future which uses carbon capture technology on coal plants since one important possibility involves the use of large quantities of oxygen, rather than air, in the combustion process. This presents the possibility of a coupling of fusion to fossil fuels with carbon capture, through the production of gases.

These links between different markets for gas products depends on the phasing of carbon capture and fusion in the market and represents a complex interaction between different energy sources which is not resolved here. It does raise interesting challenges however, overall, it still appears that the best strategy for

fusion is to target the production of electricity, even if that electricity should later be used for electrolysis or production of gases through an air separation unit.

## 7.5 FUTURE PLANS

In Materials Modelling we will continue our work to understand behaviour of bcc metals, especially ferritic and ODS steels and tungsten, particularly low temperature embrittlement and the effects of radiation damage. We will also work closely with UK Universities participating in the EPSRC-funded Materials Programme Grant (Oxford, Liverpool and Salford), in order to ensure the essential close interaction of our theory work and the Universities' experimental programme. Key activities are likely to focus on:

- Development of a quantitative model for phase stability of bcc W-Ta and W-V alloys, and investigation of the effect of Ta and V solutes on radiation point defects in W alloys;
- Further development of a discrete dislocation dynamics simulation code and application to realistic crystal simulations, with modelling of mechanical properties of iron in the high temperature limit, and code validation against micromechanical tests;
- Further development of Magnetic Cluster Expansion treatment vacancy and interstitials evolution in Fe-Cr alloys;
- Use of semi-classical atomistic models and methods for fast integration of spin-lattice dynamics (SLD) equations of motion, with application to modelling phase transitions in iron and high temperatures.

In Materials Activation and Nuclear Data and Codes, our aim is the production of a combined transport-activation nuclear data library in collaboration with European partners. We also will set in train the production of experimental data to help validate materials modelling and guide optimisation of materials and selection of priority materials for testing in IFMIF and use in the ITER Test Blanket Modules. Principal activities will be:

- Testing and improving the European Activation System (EASY) and European Activation File (EAF);
- Modernisation of the numerical and programming capabilities of the FISPACT inventory code, to realise an essentially new generation transmutation-decay code containing many new capabilities;
- Combination of EAF-2010 neutron activation cross-section library with TENDL-2010 neutron transport library to create a general single-purpose file to satisfy all radiation-transport dosimetry and activation-transmutation modelling requirements, interfacing this to Monte Carlo (MCNP) and FE (Attila) neutron transport codes for ITER and other applications;
- Setting up a programme to perform experimental study using UK-based 14MeV neutron sources in support of Fusion Materials activation / transmutation characterisation and modelling.

In our Plasma Facing Materials work, we will continue the programme to understand erosion of plasma-facing materials – in the main wall and the divertor – and the degree to which they trap fuel. The main objective is to characterise the properties of tungsten and beryllium in order to inform the ITER programme.

We will continue the programme of analysis of material removed from JET (as discussed in Section 7.3 above) and participate in future material analysis

removed from the JET ILW. Working through the JET task forces and EFDA Special Working Groups, we will compare and contrast with results from previous wall, and draw conclusions for the use of tungsten and beryllium in ITER.

Experimentally, we will continue to use the ion beam tile analysis facility at University of Sussex and to support the proposed Shrivenham/Cranfield bid to EPSRC for a successor facility capable of analysing activated beryllium.

In Technology, we intend to complete the work on identifying key impacts of pulsed operation on the engineering of DEMO. In completing EFDA tasks already awarded in 2009, we will compare H&CD systems for efficiency, real time control, materials, reliability, maintainability, health lifetime monitoring, and identify areas for further research. Also as part of this work, CCFE will develop NBI neutraliser concepts, e.g. avoidance of Cs for low work function surfaces.

We intend to take the first steps in establishing a multi-disciplinary team to integrate physics and engineering studies of systems for testing fusion power technologies and components. If and when an EU DEMO programme is established, we will bid for tasks, concentrating on CCFE target areas of blanket, divertor, H&CD and Remote Handling and Tritium technologies. We also intend to continue efforts, begun in 2009, to build collaborations with universities and industry, and support collaborative Programme Grant bids to EPSRC from UK Universities.

We will use the PROCESS code system studies to establish specification of requirements for fusion materials' performance, and the key trade-offs between development programme goals and economics/environmental performance of Fusion Energy. We will feed the results into UK and EU decision making process for technology development, including prioritisation of technology facility portfolio at CCFE. In the latter case, we will carry out a study to establish desirable technology facilities and options on the Culham site, in line with our ten-year plan as discussed with EPSRC.

Finally, we will re-evaluate ST-CTF assumptions, in the light of 2008-10 studies of nuclear testing and tritium-breeding capabilities of Culham ST-CTF concept. The aim will be to establish trade-offs between construction and operating costs of various options, and re-evaluate machine baseline size based on improved understanding of the issues.